Progress In Electromagnetics Research C, Vol. 23, 175–190, 2011

SIGE HBT DUAL-CONVERSION WEAVER-HARTLEY DOWNCONVERTERS WITH HIGH IMAGE REJECTION

J.-S. Syu, C. C. Meng*, S.-W. Yu, and Y.-H. Teng

Department of Electrical Engineering, National Chiao Tung University, 1001 Ta Hsueh Road, Hsinchu 300, Taiwan, R.O.C.

Abstract—2.4/5.7-GHz dual-band Weaver-Hartley dual-conversion downconverters are demonstrated using 0.35-μm SiGe heterojunction bipolar transistor (HBT) technology with/without a correlated local oscillator (LO) generator. In the first implementation, the correlated LO generator consists of a divide-by-two frequency divider, a frequency doubler and a single-sideband upconverter and thus LO_1 ($= 2.5 \times LO_2$) signal is generated. As a result, the downconverter with the correlated LO signals has image-rejection ratios of more than 39 dB for the first/second image signals (IRR_1/IRR_2) of the dual-conversion system at both 2.4/5.7-GHz modes while the downconverter without the correlated LO generators has a 6-dB higher conversion gain and IRR_1/IRR_2 of more than 44 dB with the same dc power consumption (excluding the LO generator). On the other hand, a 10-GHz Weaver-Hartley downconverter is demonstrated with a resonant LC load at the first-stage mixer to improve the conversion gain at high frequencies. The downconverter achieves a conversion gain of 8 dB with IRR_1/IRR_2 better than 43/40 dB.

1. INTRODUCTION

A single-conversion zero-IF (direct-conversion) dual-band system needs two separate systems including two LO generators [1]. On the other hand, with a suitable frequency planning, hardware reuse [including low-noise amplifier (LNA), mixer, and LO generator] is achievable in a dual-conversion system. For example, the second-stage mixer is reused [2] but two sets of LNAs, first-stage mixers and LO_1 generators are still required, as shown in Fig. 1(a). In [3], the dual-band

Received 29 June 2011, Accepted 12 August 2011, Scheduled 16 August 2011

* Corresponding author: Chinchun Meng (ccmeng@mail.nctu.edu.tw).

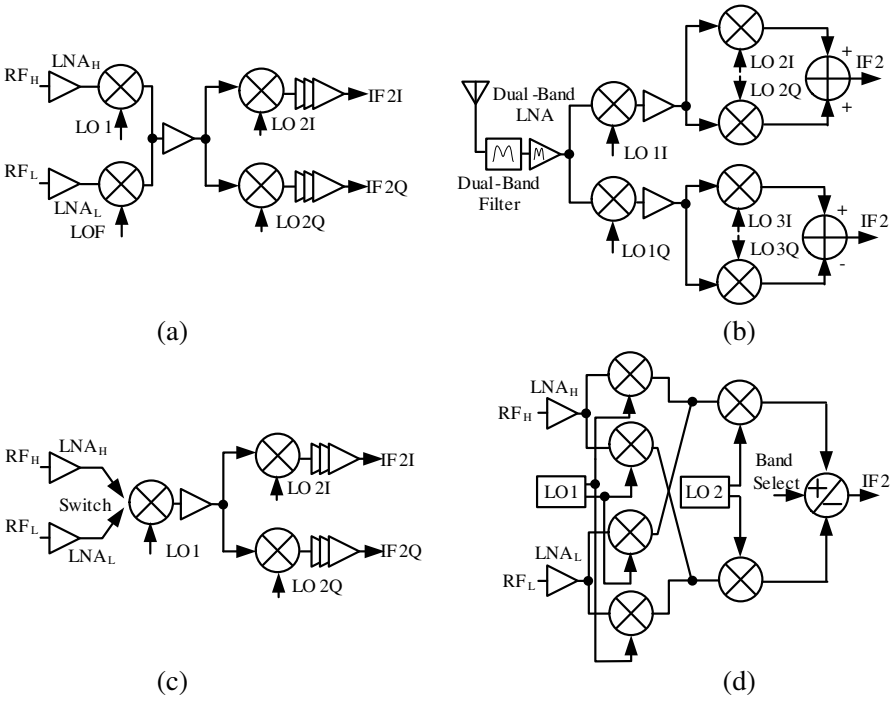

Figure 1. Block diagrams of dual-conversion receivers (a) with reused second-stage mixer (b) with reused LNA and first-stage mixer (c) with reused first- and second-stage mixers and a switchable mixer RF input stage (d) with reused first- and second-stage mixers.

concurrent LNA and the first-stage mixer are reused. The two signal bands after the first downconversion should be downconverted to baseband by two different LO_2 signals, as shown in Fig. 1(b). That is, at least three LO generators should be utilized. Further, as shown in Fig. 1(c), the first- and second-stage mixers are reused with an RF input switchable transconductance stage while the LO_1 signal is set approximately but not exactly halfway between the two operation bands [4]. Therefore, the first-downconverted signals are near and can be selected by choosing proper LO_2, like a wideband IF architecture. However, the LO_1 and LO_2 frequencies can not be correlated for this frequency planning. Finally, fully reused first/second-stage mixers are demonstrated while the LO_1 is set exactly halfway between the two bands, as shown in Fig. 1(d) [5]. After the first downconversion, the two bands are located at either positive or negative frequency spectrum. Thus, the output signal can be selected in the second-stage mixer.

In addition, a dual-band antenna [6] and a dual-band pre-selection filter [7] are also widely used for a hardware-reuse dual-band system.

To avoid the severe flicker noise, dc offset and IIP_2 problems of a direct-conversion receiver [8, 9], a low-IF receiver is also widely chosen and implemented [10–13]. Instead of solving those problems in a direct-conversion system, filtering or suppressing the image signals becomes the most important issue of a low-IF receiver because the final IF frequency is not zero. In this paper, a 2.4/5.7-GHz dual-band low-IF system for WLAN 802.11 a/g applications is demonstrated. Since the low-IF architecture keeps the IF frequency flexible, the LO_1 and LO_2 can be set as the fractional multiple of each other. That is, the two LO signals can be generated by one source. The correlated LO signals maintain excellent image-rejection performance because the phase errors at the LO_1 and LO_2 differential-quadrature signals can be kept the same [14] by a good LO generator.

On the other hand, in a high-frequency receiver, the LO_1/LO_2 signals should be carefully designed. For example, a high IF_1 frequency ($\omega_{IF1} = \omega_{RF} - \omega_{LO1}$) helps filter the first image signal because the image signal is $2\omega_{IF1}$ away from the RF signal. However, if ω_{IF1} is very high, the quadrature accuracy of LO_2 signal is difficult to maintain and the output low-pass bandwidth of the RC load at the first-stage mixer is difficult to achieve [15]. Thus, a parallel LC tank resonated at ω_{IF1} can be chosen as the load of the first-stage mixer to improve the system conversion gain.

2. WEAVER-HARTLEY ARCHITECTURE

The dual-conversion low-IF system combines the Weaver architecture [14, 16, 17] and Hartley architecture [18]. The former is a complex dual-conversion topology which removes the first image signal by the frequency-shifting mechanism while the latter is a complex down conversion with a complex polyphase filter to remove the second image. The Weaver system in this work consists of a single-quadrature first-stage complex mixer and a double-quadrature second-stage complex mixer as shown in Fig. 2. A single-quadrature complex mixer includes two real mixers with either a quadrature RF or LO input while the other is kept differential. A double-quadrature complex mixer includes four real mixers with both LO and RF signals being quadrature.

In a Weaver system, received signals are twice downconverted to a low-IF band by the LO_1/LO_2 signals. The angular frequencies of the desired RF, first image (IM_1), and second image (IM_2), LO_1, and LO_2 signals are denoted as ω_{RF}, ω_{IM1}, ω_{IM2}, ω_{LO1} and ω_{LO2}, respectively. The angular frequencies of the IF signal after the first

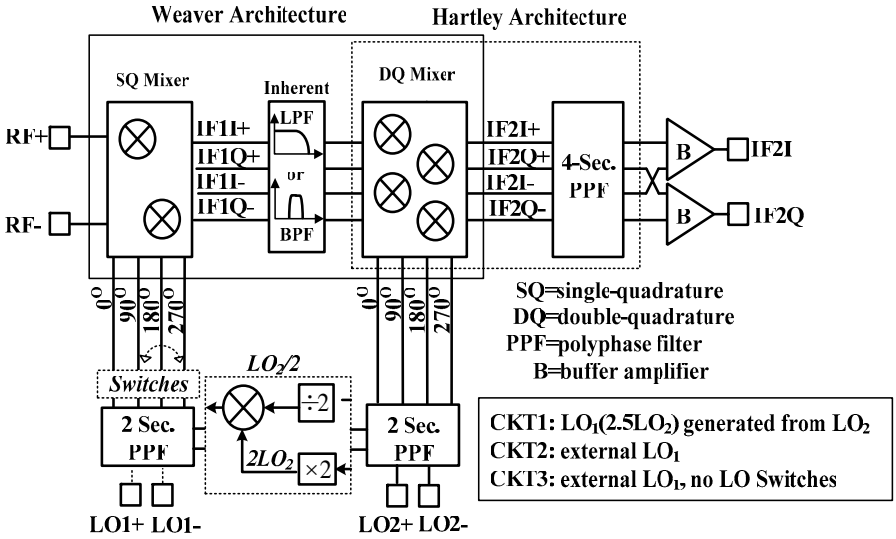

Figure 2. Block diagram of a single/dual-band dual-conversion Weaver-Hartley low-IF system.

and second downconversions are defined as ω_{IF1} and ω_{IF2}, respectively. The relations of the signals defined above can be expressed as:

$$\begin{cases} \omega_{RF} - \omega_{LO1} = \omega_{LO1} - \omega_{IM1} = \omega_{IF1} \\ \omega_{RF} - (\omega_{LO1} + \omega_{LO2}) = (\omega_{LO1} + \omega_{LO2}) - \omega_{IM2} = \omega_{IF2} \\ \omega_{IF1} = \omega_{LO2} + \omega_{IF2} \end{cases} . \quad (1)$$

The wire connection of the Weaver system with detailed mathematical analyses is shown in Fig. 3. Fig. 3(a) indicates the results at each node of the Weaver system when the input signals are RF and IM_1. Both signals are converted to the same IF_1 frequency (ω_{IF1}) but with opposite signs of the quadrature signals after the first downconversion. The high-frequency term ($2\omega_{LO1} + \omega_{IF1}$) can be eliminated by the low-pass/band-pass nature of the first-stage mixer. The other two signals entering the second-stage mixers are downconverted to ω_{IF2} and ($2\omega_{IF1} - \omega_{IF2}$) bands, respectively. Therefore, the shifted-out image signal can be easily filtered-out by the low-pass filter at IF_2 stage [14].

On the other hand, the RF and IM_2 signals are downconverted to ω_{IF1} and ($\omega_{IF1} - 2\omega_{IF2}$), respectively, after the first downconversion, as shown in Fig. 3(b). The two signals are still very close and difficult to be separated by a narrow-band filter. After the second conversion, the two signals locate at the same frequency (ω_{IF2}) but with opposite

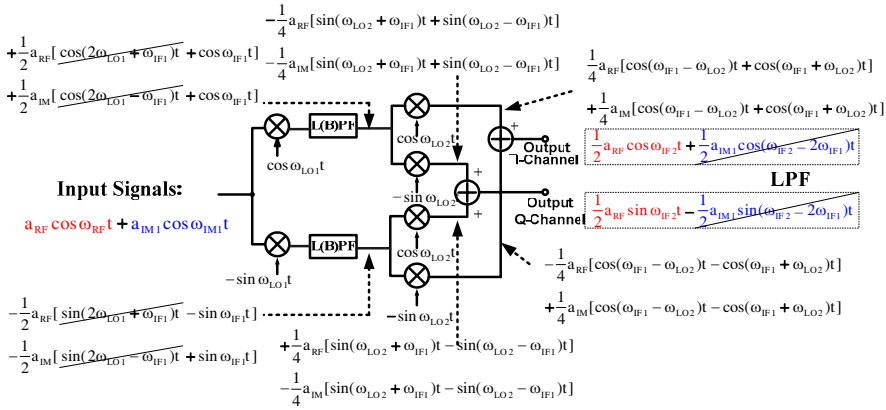

(a)

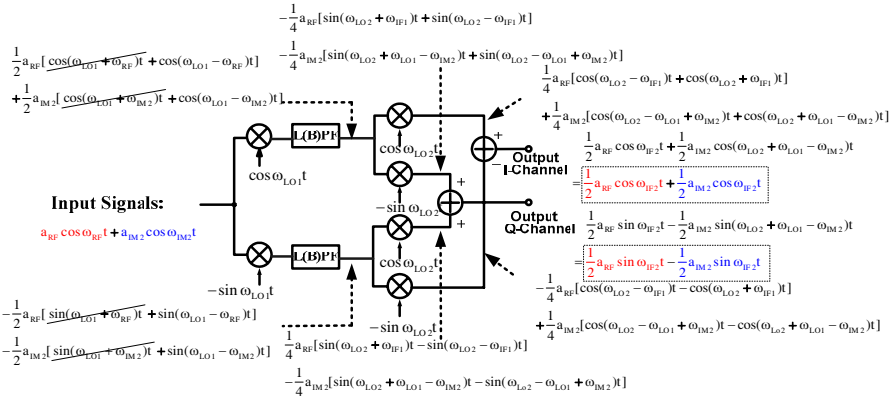

(b)

Figure 3. Block diagram of the Weaver architecture, (a) when input signals are desired RF signal and first image signal, (b) when input signals are desired RF signal and second image signal.

signs of quadrature signals. That is, the Weaver system can reject the IM_1 but not the IM_2. To solve this problem, a polyphase filter is cascaded after the Weaver system because the polyphase filters can reject the negative-frequency signal but pass the positive-frequency signal [13]. As a result, the image signals at the negative spectrum can be highly rejected. The second-stage complex mixers with the subsequent polyphase filter can be called the Hartley system.

3. CIRCUIT DESIGN AND EXPERIMENTAL RESULTS

Three implementations are proposed in this paper. First of all, a 2.4/5.7-GHz dual-band Weaver-Hartley downconverter with a correlated LO generator is introduced while the second implementation is a dual-conversion system with separate quadrature LO generators for LO power optimization. Finally, a resonant LC load is utilized at the first-stage mixer to improve the overall gain/noise for a 10-GHz downconverter.

3.1. 2.4/5.7-GHz Dual-band Weaver-Hartley Downconverter with a Correlated LO Generator

For a dual-band dual-conversion low-IF receiver, the angular frequency relations are given below:

$$\begin{cases} \omega_{RFH}(\omega_{IM1L}) - \omega_{LO1} = \omega_{LO1} - \omega_{IM1H}(\omega_{RFL}) = \omega_{IF1} \\ \omega_{RFH} - (\omega_{LO1} + \omega_{LO2}) = (\omega_{LO1} + \omega_{LO2}) - \omega_{IM2H} = \omega_{IF2} \\ \omega_{IM2L} - (\omega_{LO1} - \omega_{LO2}) = (\omega_{LO1} - \omega_{LO2}) - \omega_{RFL} = \omega_{IF2} \\ \omega_{IF1} = \omega_{LO2} + \omega_{IF2} \end{cases} \tag{2}$$

where the suffix H and L represent high-frequency and low-frequency operation modes, respectively.

That is, for a 2.4/5.7-GHz dual-band system in this work, $f_{RFH} = f_{IML} = 5.7\,\text{GHz}$, $f_{RFL} = f_{IMH} = 2.4\,\text{GHz}$. Thus, $f_{LO2} = 1.62\,\text{GHz}$, $f_{LO1} = 2.5 \times f_{LO2} = 4.05\,\text{GHz}$, and $f_{IF2} = 30\,\text{MHz}$.

The block diagram of the 2.4/5.7-GHz Weaver-Hartley downconverter is shown in Fig. 2. A Gilbert mixer consists of two current-steering differential amplifiers and thus employing SiGe HBTs for the Gilbert mixer cell has the advantages of low LO power and high conversion gain. A high conversion gain helps suppress the noise contribution of the following stages, especially the cascaded polyphase filter, to achieve a better dynamic range. The schematic of a Gilbert mixer with source degeneration employed at the single-quadrature first downconversion is shown in Fig. 4(a). Fig. 4(b) shows the second-stage Gilbert mixers with output in-phase/anti-phase connections for an addition/subtraction function to realize the complex mixing operation in a double-quadrature second downconversion. The IF common-drain buffer amplifiers are employed to facilitate 50-Ω measurements.

Moreover, an LO generator generates both differential-quadrature LO_1 and LO_2 signals. The LO_1 signal is generated from LO_2 by a frequency multiplier consisting of a frequency doubler ($\times 2$) and a frequency divider ($\div 2$) and a single-sideband (SSB) upconverter [19, 20]. After the mixing operation of an SSB upconverter, the LO_1 ($= 2.5 \times \text{LO}_2$) signal is thus generated. Both

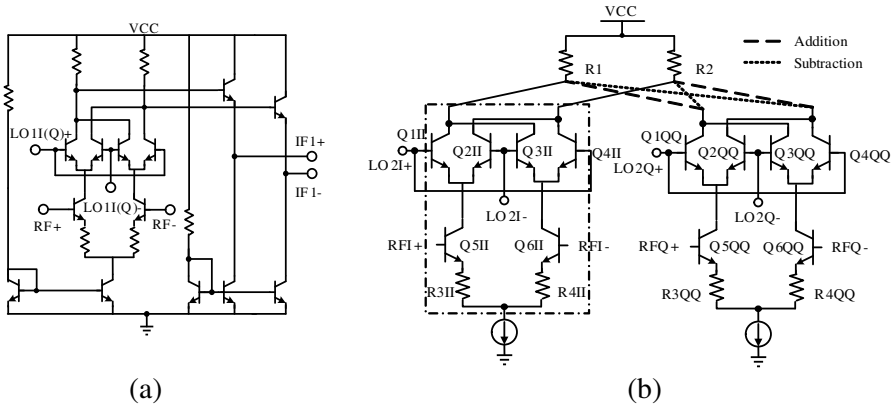

Figure 4. Schematic of (a) the first-stage Gilbert mixer, (b) the second-stage mixer.

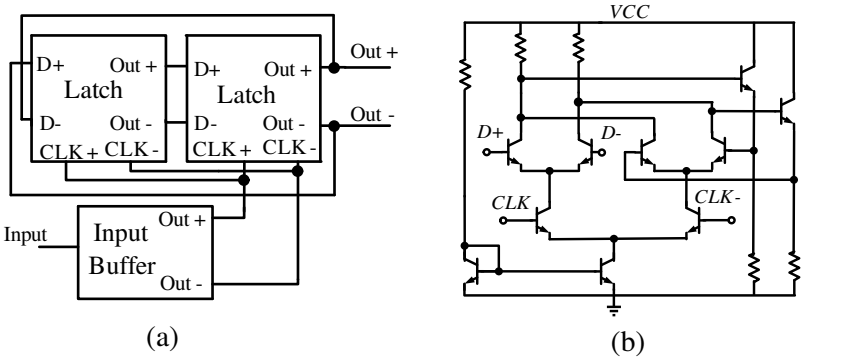

Figure 5. (a) Block diagram of the static divide-by-two divider, (b) the D-latch cell used in the divider.

differential-quadrature signals of the LO_1 and LO_2 are generated by a two-section polyphase filter with the center frequency of 4.05 and 1.62 GHz, respectively. Fig. 5(a) shows the block diagram of the static frequency divider consisting of two D-latches realized by emitter-coupled logic. The schematic of the D-latch, consisting of the sample and hold stages, is shown in Fig. 5(b). Instead of using a simple cross-coupled pair, the common-collector configuration is inserted into the positive feedback loop at the hold stage to achieve a wider output swing.

The schematic of the multiplier is shown in Fig. 6(a). Following the Equation

$$\cos\omega_1 t \times \sin\omega_2 t + \sin\omega_1 t \times \cos\omega_2 t = \sin(\omega_1 + \omega_2)t, \qquad (3)$$

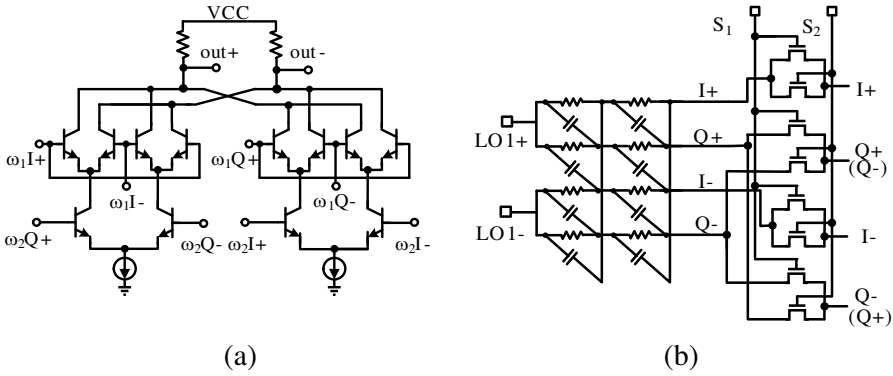

Figure 6. (a) Schematic of a multiplier which can be utilized as a single-sideband upconverter and a frequency doubler, (b) schematic of a two-section polyphase filter with following four switching pairs.

the multiplier is an SSB upconverter if $\omega_1 \neq \omega_2$ and two input signals have the perfect quadrature phase. On the other hand, the half circuit of Fig. 6(a) is a simple frequency doubler if $\omega_1 = \omega_2 = \omega_0$. The output signal has a non-50% duty cycle due to the phase delay between the two levels of current switching cores. Using the compensated frequency doubler (i.e., full circuit shown in Fig. 6(a)), truly balanced $2\omega_0$ output with 50% duty cycle is thus obtained.

In the complex mixer topology of the first stage, the mixing operation leads to the frequency spectrum right-shifting, i.e., $\omega_{IF1} = -\omega_{RF} + \omega_{LO1}$, if the differential-quadrature LO_1 has the positive output sequence (0°, 90°, 180° and 270°). On the other hand, if the polarity of the LO_1 is reversed (0°, 270°, 180° and 90°), the output spectrum is left-shifting, i.e., $\omega_{IF} = \omega_{RF} - \omega_{LO1}$. By setting the LO_1 frequency at 4.05 GHz, halfway between 2.4 GHz and 5.7 GHz, the 2.4-GHz receiving mode employs the positive LO_1 sequence while the 5.7-GHz receiving mode employs the negative LO_1 sequence. As a result, the outputs at the first stage are both downconverted to 1.65 GHz with positive I/Q output sequence when the desired signal is received at both modes. Therefore, the dual-band operation can be achieved. The schematic of the switching pairs cascaded after a two-section polyphase filter is shown in Fig. 6(b). When $(S_1, S_2) = (L, H)$, the 5.7-GHz band is selected. On the other hand, the 2.4-GHz band is chosen if $(S_1, S_2) = (H, L)$.

Figure 7(a) shows the die photo of the 2.4/5.7-GHz dual-band dual-conversion downconverter with a correlated LO signal generator and the die size is $1.63 \times 1.52\,\text{mm}^2$. On-wafer measurement is employed

for the RF performance. Fig. 7(b) shows the conversion gain (CG) and the single-sideband noise figure (SSB NF) of 2.4/5.7-GHz bands at a 3-V supply. The CG is 5/4 dB while the NF is about 20 dB for 2.4/5.7-GHz band when the LO power is 2 dBm. Besides, the image-rejection ratios for the first/second image signals (IRR_1/IRR_2) for 2.4-GHz band are shown in Fig. 8. The IRR_1 is above 40 dB and is flat due to the frequency shifting mechanism. When compared with the IRR_1, the IRR_2 is 44 dB within a narrow band from 15 to 45 MHz due to the frequency response of the four-section polyphase filter following the

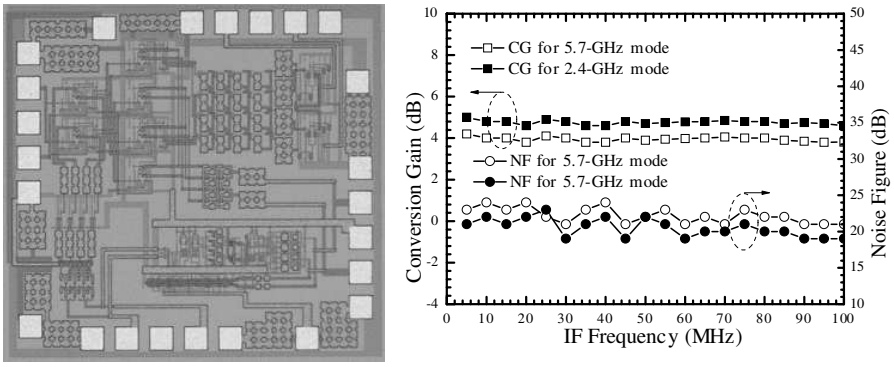

Figure 7. (a) Die photo, (b) conversion gain and single-sideband noise figure of the dual-band Weaver-Hartley downconverter with a correlated LO signal generator.

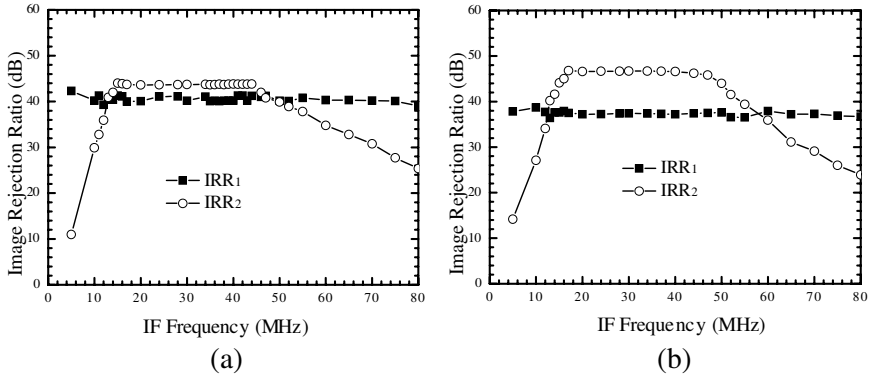

Figure 8. Image rejection ratios of the dual-band Weaver-Hartley downconverter with a correlated LO signal generator (a) at 2.4-GHz mode, (b) at 5.7-GHz mode.

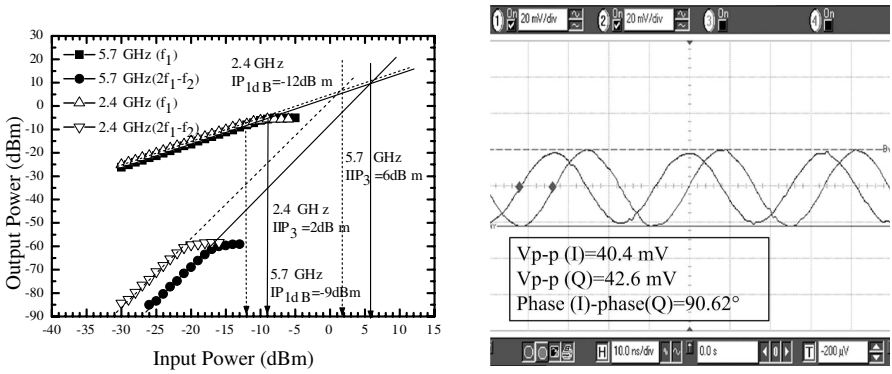

(a) (b)

Figure 9. (a) Power performance, (b) output I/Q waveforms of the dual-band Weaver-Hartley downconverter with a correlated LO signal generator.

second-stage mixers. On the other hand, the IRR_1 and IRR_2 are 39 and 46 dB within the IF bands from 15 to 45 MHz for the 5.7-GHz mode as shown in Fig. 8(b). Fig. 9(a) shows the power performance of both bands. The $IP_{1\,dB}$ is $-12/-9$ dBm while the IIP_3 is 2/6 dBm for 2.4/5.7-GHz band when $IF = 30$ MHz. The output waveform of both I/Q channels are shown in Fig. 9(b) and the figure shows 0.46 dB magnitude mismatch and 0.62° phase error.

3.2. 2.4/5.7-GHz Dual-band Weaver-Hartley Downconverter with Separate LO Generators

The block diagram of the 2.4/5.7-GHz Weaver-Hartley downconverter with separate LO quadrature generators is also shown in Fig. 2. The only difference from the former section is the use of two separate two-section polyphase filters for external LO_1 and LO_2 inputs. The die photo is shown in Fig. 10(a) and the die size is $1.7 \times 1.4\,mm^2$.

Figure 10(b) shows the CG and SSB NF of the downconverter with respect to the IF frequency. The CG is 11/10 dB and the NF is about 19/18 dB for 2.4/5.7-GHz band. The downconverter reaches the peak gain when LO_1 power is 13 dBm and LO_2 power is 5 dBm. The IRRs for 2.4/5.7 GHz band are 45/44 dB for the first image and 50/48 dB for the second image as shown in Fig. 11. The power performance is shown in Fig. 12(a). The $IP_{1\,dB}$ is $-16/-15$ dBm while the IIP_3 is $-3/-2$ dBm for 2.4/5.7-GHz band. The output I/Q signals have 0.1 dB gain mismatch and 0.7° phase error as shown in the output waveforms of Fig. 12(b).

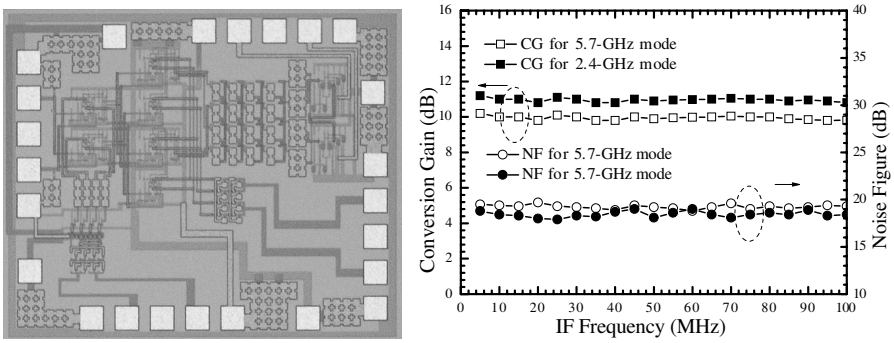

Figure 10. (a) Die photo (b) conversion gain and noise figure of the 2.4/5.7-GHz Weaver-Hartley downconverter with separate LO generators.

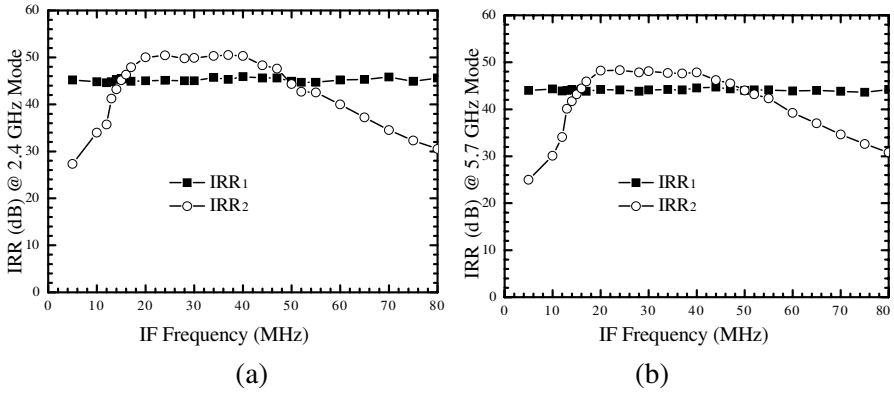

Figure 11. Image rejection ratio of the dual-band Weaver-Hartley downconverter with separate LO generators (a) at 2.4-GHz mode, (b) at 5.7-GHz mode.

3.3. 10-GHz Weaver-Hartley Downconverter with a Resonant LC Load

For a single-band Weaver-Hartley downconverter, the LO_1 switches in Fig. 2 is not needed. In this section, the RF frequency is targeted at 10 GHz and the resulting LO_1/LO_2 is around 6/4 GHz, respectively. Since the conversion gain of an active mixer is determined by the input trasconductance stage and the output load. Conventionally, the load resistance and the parallel load capacitance including parasitic capacitances determine the IF output low-pass bandwidth. Therefore,

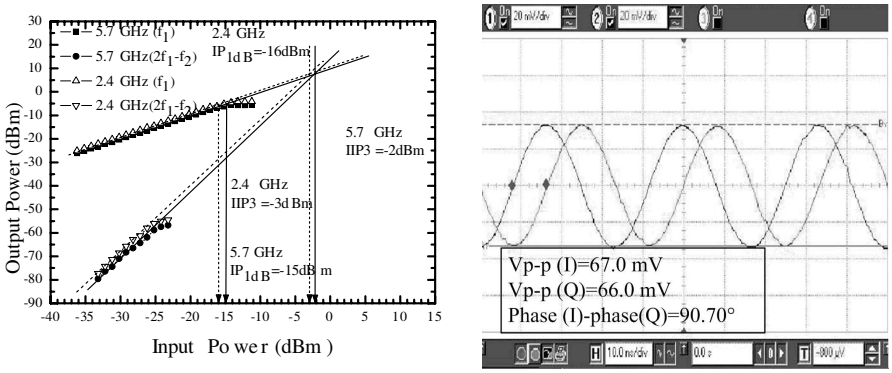

(a) (b)

Figure 12. (a) Power performance, (b) output I/Q waveforms of the dual-band Weaver-Hartley downconverter with separate LO generators.

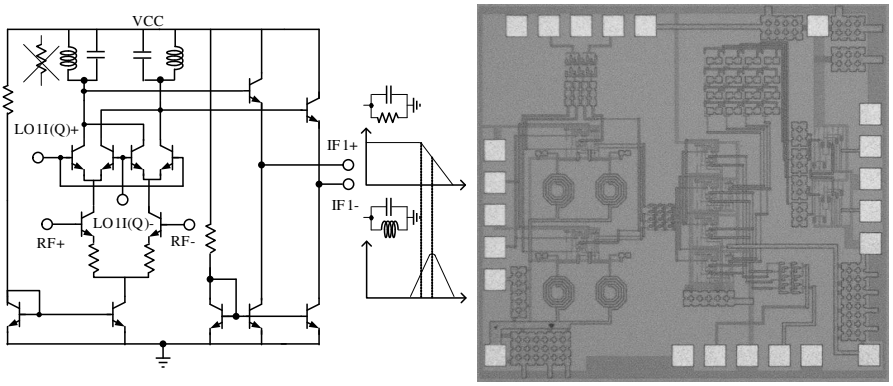

(a) (b)

Figure 13. (a) Schematic of the first-stage Gilbert mixer with a resonant LC load, (b) die photo of the 10-GHz Weaver-Hartley downconverter.

the transistor sizes should be optimized and the output load resistance should be sufficiently low to increase the IF bandwidth at the cost of the conversion gain. However, a parallel LC tank resonated at ω_{IF1} (around 4 GHz, which is difficult to be achieved by a low-pass response of an RC load) is applied at the first-stage mixer to increase the conversion gain at a high IF frequency, as shown in Fig. 13(a). In addition, each quadrature LO_1 and LO_2 is generated by a two-section polyphase filter.

A die photo of the 10-GHz Weaver-Hartley downconverter is shown in Fig. 13(b) and the die size is $1.9 \times 1.73\,\text{mm}^2$. A conversion gain reaches a flat region when the LO_1 and LO_2 power are larger than 6 and 0 dBm, respectively. The CG of 8 dB and SSB NF of around 18 dB when IF frequency (ω_{IF2}) ranges from 15 to 100 MHz, which is also the image-rejection band are shown in Fig. 14(a). Fig. 14(b) shows both IRR_1 and IRR_2. The IRR_1 is around 43 dB (maximum: 48 dB) within 100 MHz. The IRR_2 is better than 40 dB (maximum: 52 dB) within 15 to 100 MHz and is better than 45 dB within 25 to 90 MHz. The IP_{1dB}

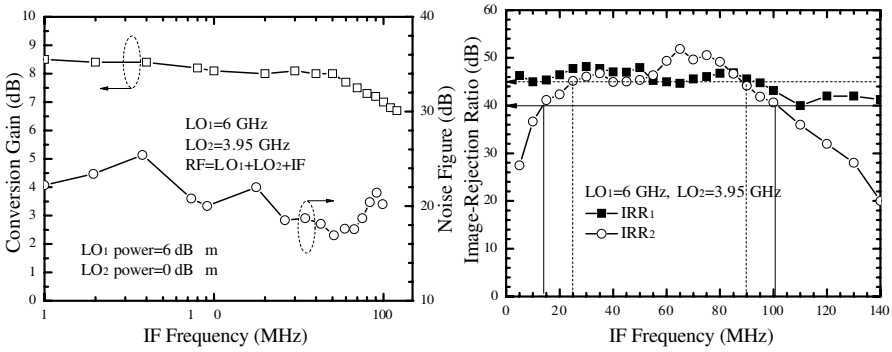

(a) (b)

Figure 14. (a) Conversion gain and single-sideband noise figure with respect to the IF frequency, (b) image-rejection ratio of the 10-GHz Weaver-Hartley downconverter.

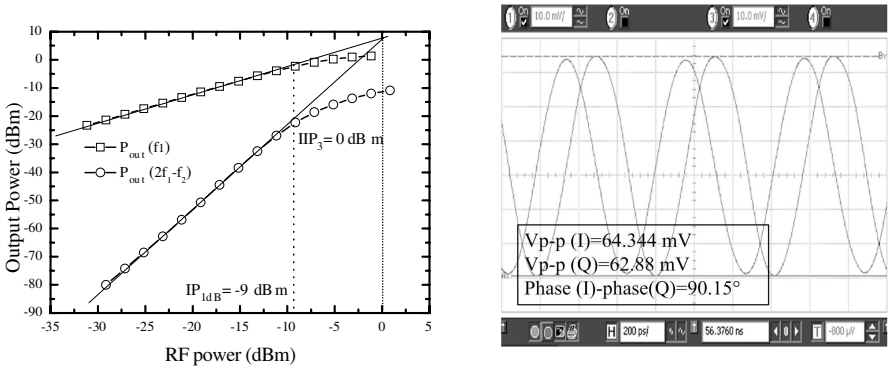

(a) (b)

Figure 15. (a) Power performance, (b) I/Q output waveforms of the 10-GHz Weaver-Hartley downconverter.

Table 1. Performance summary and comparison.

Reference	CKT1	CKT2	CKT3	[5]	[19]
f_{RF} (GHz)	2.4/5.7	2.4/5.7	10	0.9/1.8	2.4/5.7
f_{LO1}/f_{LO2} (GHz)	4.05/1.62	4.05/1.62	6/4	1.35/0.45	4.05/1.62
CG (dB)	5/4	11/10	8	23/23 (Av)	9/8
SSB-NF (dB)	20/20	19/18	18	4.7/4.9	23/25
IRR_1 (dB)	40/39	45/44	> 43 (48 max.)	40/36	40/40
IRR_2 (dB)	44/46	50/48	> 40 (52 max.)	N.A.[a]	44/46
IF Bandwidth (MHz)	15–45	20–40	15–100	N.R.	15–45
Supply Voltage (V)	3	4	3.3	3	1.8
Chip Size (mm^2)	1.63×1.52	1.7×1.4	1.90×1.73	1.54×1.37	2×2
Technology	0.35-μm SiGe HBT			0.6-μm CMOS	0.18-μm CMOS

[a] $IF_2 = 0$, no second image.

and IIP_3 are -9 and 0 dBm as shown in Fig. 15(a) and Fig. 15(b) shows I/Q output waveforms of the downconverter with 0.15° phase error and 0.2 dB amplitude mismatch. The circuit performance of three implementations is summarized and compared with other state-of-the-art dual-band receivers in Table 1 [5, 19].

4. CONCLUSION

Two 2.4/5.7-GHz dual-band Weaver-Hartley dual-conversion downconverters are demonstrated in this paper using 0.35-μm SiGe HBT technology. A correlated LO generator is applied in one implementation while the other circuit utilizes two separate LO quadrature generators. The correlated LO signals maintain excellent image-rejection performance of the dual-conversion system. However, 6 dB improvement is obtained by using separate LO generators with an optimized LO input power. In addition, a 10-GHz Weaver-Hartley downconverter is demonstrated with a resonant LC load at the first-stage mixer to improve the overall conversion gain.

ACKNOWLEDGMENT

This work is supported by National Science Council of Taiwan, Republic of China under contract numbers NSC 98-2221-E-009-033-MY3, NSC 98-2221-E-009-031 and NSC 98-2218-E-009-008-MY3, and by MoE ATU Program under contract number 95W803. The authors would like to thank National Chip Implementation Center (CIC) for technical support.

REFERENCES

1. Behzad, A., et al., "A fully integrated MIMO multiband direct conversion CMOS transceiver for WLAN applications (802.11n)," *IEEE J. Solid-state Circuits*, Vol. 42, No. 12, 2795–2808, Dec. 2007.
2. Zargari, M., et al., "A single-chip dual-band tri-mode CMOS transceiver for IEEE 802.11a/b/g wireless LAN," *IEEE J. Solid-state Circuits*, Vol. 39, No. 12, 2239–2249, 2004.
3. Hashemi, H. and A. Hajimiri, "Concurrent multiband low-noise amplifiers — Theory, design, and applications," *IEEE Trans. Microw. Theory Tech.*, Vol. 50, No. 1, 288–301, Jan. 2002.
4. Ahola, R., et al., "A single-chip CMOS transceiver for 802.11a/b/g wireless LANs," *IEEE J. Solid-state Circuits*, Vol. 39, No. 12, 2250–2258, 2004.
5. Wu, S. and B. Razavi, "A 900-MHz/1.8-GHz CMOS receiver for dual-band applications," *IEEE J. Solid-state Circuits*, Vol. 33, No. 12, 2178–2185, 1998.
6. Panda, J. R. and R. S. Kshetrimayum, "A printed 2.4 GHz/5.8 GHz dual-band monopole antenna with a protruding stub in the ground plane for WLAN and RFID applications," *Progress In Electromagnetics Research,* Vol. 117, 425–434, 2011.
7. Chiou, Y.-C., P.-S. Yang, J.-T. Kuo, and C.-Y. Wu, "Transmission zero design graph for dual-mode dual-band filter with periodic stepped-impedance ring resonator," *Progress In Electromagnetics Research*, Vol. 108, 23–36, 2010.
8. Abidi, A. A., "Direct-conversion radio transceivers for digital communications," *IEEE J. Solid-state Circuits*, Vol. 30, No. 12, 1399–1410, 1995.
9. Elahi, I. and K. Muhammad, "Asymmetric DC offsets and IIP2 in the presence of LO leakage in a wireless receiver," *RFIC Symp. Dig. Papers*, 313–316, 2002.

10. Fang, S. J., A. Bellaouar, S. T. Lee, and D. J. Allstot, "An image-rejection downconverter for low-IF receivers," *IEEE Trans. Microw. Theory Tech.*, Vol. 53, No. 2, 478–487, 2005.
11. Wu, C.-Y. and C.-Y. Chou, "A 5-GHz CMOS double-quadrature receiver front-end with single-stage quadrature generator," *IEEE J. Solid-state Circuits*, Vol. 39, No. 3, 519–521, 2004.
12. Tadjpour, S., E. Cijvat, E. Hegazi, and A. A. Abidi, "A 900-MHz dual-conversion low-IF GSM receiver in 0.35-μm CMOS," *IEEE J. Solid-state Circuits*, Vol. 36, No. 12, 1992–2002, 2001.
13. Behbahani, F., Y. Kishigami, J. Leete, and A. A. Abidi, "CMOS mixers and polyphase filters for large image rejection," *IEEE J. Solid-state Circuits*, Vol. 36, No. 6, 873–887, 2001.
14. Wu, T.-H. and C. C. Meng, "5.2/5.7 GHz 48 dB image rejection GaInP/GaAs HBT weaver downconverter using LO frequency quadrupler," *IEEE J. Solid-state Circuits*, Vol. 41, No. 11, 2468–2480, 2006.
15. Syu, J.-S., C. C. Meng, Y.-H. Teng, and G.-W. Huang, "X-band weaver-hartley low-IF downconverter with a resonant LC load," *Asia Pacific Microwave Conference (APMC)*, 1168–1171, Dec. 2009.
16. Weaver, D., "A third method of generation and detection of single-sideband signals," *Proceedings of the IRE*, 1703–1705, 1956.
17. Rudell, J. C., J.-J. Ou, T. B. Cho, G. Chien, F. Brianti, J. A. Weldon, and P. R. Gray, "A 1.9-GHz wide-band IF double conversion CMOS integrated receiver for cordless telephone applications," *IEEE J. Solid-state Circuits*, Vol. 32, No. 12, 2071–1088, 1997.
18. US 1,666,206, "Modulation System," Apr. 17, 1928.
19. Meng, C. C., T.-H. Wu, J.-S. Syu, S.-W. Yu, K.-C. Tsung, and Y.-H. Teng, "2.4/5.7-GHz CMOS dual-band low-IF architecture using Weaver-Hartley image-rejection techniques," *IEEE Trans. Microw. Theory Tech.*, Vol. 57, No. 3, 552–561, Mar. 2009.
20. Syu, J.-S., C. C. Meng, and G.-W. Huang, "Dynamic range reduction due to RF and image signal co-existence in a highly-merged 2.4/5.7-GHz dual-band low-IF downconverter," *IEEE MTT-S Int. Microw. Symp. Dig.*, 1016–1019, May 2010.